ABSTRACT

HOWELL, TRAVIS LYNN. The Benefits and Applications of Unmanned Aerial Systems (UAS) to Natural Resources & Forest Management. (Under the direction of Dr. James McCarter and Dr. Stacy Nelson.)

Forestry, as well as the natural resources field, can be faced with the challenge of gathering spatial data in areas that are nearly impossible for humans to access, or inventory in reasonable time. Standard boots on the ground data collection in densely vegetated stands, conducting large site inspections, or hand derived wood pile volume estimations can result in low productivity and controversial data. Unmanned aerial systems (UAS) and the miniaturization of remote sensing devices have proved to be cost-effective tools that allow for site reconnaissance and highly accurate three-dimensional (3D) mapping. The ability to view pairs of hard copy photography in stereo has existed for decades, but thanks to recent structure from motion (SfM) computer programs, multiple pairs of digital photos acquired via UAS can be stitched together to generate a corresponding 3D point cloud. Additionally, nearly any sensor can be mounted on the UAS for the ability to conduct instantaneous remote sensing.

The Benefits and Applications of Unmanned Aerial Systems (UAS) to Natural Resources &
Forest Management

by
Travis Lynn Howell

A thesis submitted to the Graduate Faculty of
North Carolina State University
in partial fulfillment of the
requirements for the Degree of
Master of Science

Forestry & Environmental Resources

Raleigh, North Carolina

2017

APPROVED BY:

_____   _____
Dr. James McCarter   Dr. Stacy Nelson
Committee Co-Chair   Committee Co-Chair
Minor Representative

_____
Dr. Joseph Roise
Committee Member

BIOGRAPHY

Travis Howell graduated from North Carolina State University in 2014 with a B.S. in Forest Management and minor in Agriculture Business Management. He worked in the private sector as a procurement forester in Eastern North Carolina before heading back to NCSU to get his M.S. in Forestry and GIS with a concentration in the application of unmanned aerial systems (UAS) in Forestry and Natural Resources. Currently he is employed by WithersRavenel as a GIS Technician and assisting with the research and development of applying UAS's in both civil and environmental fields.

TABLE OF CONTENTS

LIST OF TABLES

LIST OF FIGURES

Chapter 1

1.0 Introduction

Recently the use and exploration of remotely piloted systems attached with various remote

sensing devices has been on the rise in natural resources fields. The terms Unmanned Aerial

System (UAS) and Unmanned Aerial Vehicle (UAV) are sometimes used as synonyms;

however, in correct usage as stated by the Federal Aviation Administration (FAA), UAV

only describes the aerial platform, not the system as a whole, therefore this study will use the

term UAS.

Various versions of UAS have been around for decades, but until recently, they have been

too expensive or incapable of acquiring useful remotely-sensed data without requiring

extensive prior knowledge (Zhou and Zang 2007). Commercial and research applications of

UAS's have recently gained momentum due to technological advancements that have

reduced costs and increased platform efficiencies. Its incredible potential is now feasible

owing to battery-integrated power management, lightweight brushless rotors, and miniature

remote sensing devices. This allows for light UAS's to be able to fly and acquire data that

can be processed in real-time or in post-processing that delivers position orientated

parameters up to cm-level precision. (Rehak et al., 2013). Common applications that have

emerged include coverage analysis for cellular networks, timber harvest auditing, natural

disaster inspection, hydrology management, archaeological surveys, and vegetation

monitoring (Berni et al. 2009; Breckenridge et al. 2011; Chiabrando et al. 2009; Goddemeier

et al. 2010; Themistocleous et al. 2015; Wallace et al. 2012). These studies may use image

matching and photogrammetric techniques, which allow generation of high-density point clouds from the very high-resolution photos collected by an UAS (Wallace et al. 2012). Initially, images are acquired at the proper altitude and angle (oblique and/or nadir), with an appropriate percent of overlap in order to be correctly stitched together to create a high-resolution three-dimensional (3D) point cloud. Then, structure from motion (SfM) programs are used to generate, view, and manipulate high-resolution point clouds and mosaics that can be spatially referenced to centimeter-level accuracy, if ground control points (GCP) are available. Even without placing GCP's, a mosaic can contain relatively accurate X (latitude) & Y (longitude) data if the photos used to generate it were able to be georeferenced. Generally, Z (altitude) values used for 3D modeling will vary greatly across the model without the aid of evenly distributed GCP's. Once the mosaic is orthorectified within an SfM program via GCP points, the mosaic is transitioned into a referenced orthophoto.

1.1 UAS History

To properly understand where UAS technology is headed, it is important to understand its origin. Often, the name 'drone' may be used as its originality was emphasized in the early 1900's when the Royal Navy was perfecting a remote-control aircraft for target practice. The de Havilland 'DH-82B', also known as the Queen Bee (Figure 1) was one of the first modern day remotely piloted aircraft and was used for aerial target practice. As all aircraft developed after that were in homage to the Queen Bee, it was appropriate to title them as drones. Ben

Zimmer from the Wall Street Journal writes "Since old English, 'drone' has referred to a male honey bee whose only role is to mate with the queen bee".

Figure 1: de Havilland "DH-82B" Queen Bee and remote pilot base station

1.2 FAA Regulations

With advancement in airborne data collection also comes the responsibility of operating and controlling a moving system that is in public airspace. It has been noted that the greatest limitation of UAS's lies in the absence of legislation and regulation for operation in non-segregated airspace. The problem posed by allowing unmanned aircraft to operate in the same 'civil' airspace as traditional aircraft has been a controversial subject among pilots, airlines and aviation safety authorities for several years (BIGS 2012). Micro/Mini UAS's are classified as very low altitude (VLA) systems operating in Class G airspace and are typically bound by: altitudes less than 400ft, the operator always being in visual contact with the

aircraft, daylight conditions only, and outside of 5 nautical miles from any airport, heliport, seaplane base, spaceport, or other location with aviation activities. As of Dec. 21, 2015, the FAA requires all owners of micro/mini UAS's or aircraft weighing between 0.55 and 55 pounds to register the craft before flying. The online certification form (Aircraft Registration Application, AC Form 8050-1) by the FAA can result in a unique identification number owners must affix to the UAS prior to use. In order to use UAS for commercial use, the pilot has to obtain a Part 107 certification that certifies pilots of the situational awareness and aeronautical responsibilities to ensure safe flights. Commercial use can be defined as anything other than a recreational activity, or if the data is being collected for a purpose other than personal enjoyment. Some state agencies such as the North Carolina Department of Transportation (NCDOT) require UAS operators to obtain an additional permit by completing a simple online knowledge test before commercial or government UAS operations occur.

1.3 UAS Platforms

Under the title of micro/mini UAS (hereafter referred to only as UAS) there are four main categories that determine the platforms versatility: flight range, vertical takeoff ability, battery endurance, and maximum takeoff weight (MTOW). Typically, there are two main airframe configurations: fixed wing and multirotor aircraft. A fixed-wing aircraft has immovable wings that require some type of runway to take off and land, or can be catapult launched. This type of platform is best suited for large landscape inventory, similar to

agriculture fields where there are limited over-head obstructions and soft landing areas. Most of the time sensors are mounted on the belly of the aircraft and only offer data acquisition in the nadir position.

A multirotor copter (informal term for helicopter) refers to an aircraft that takes off and lands vertically. Multirotor copters have the ability to hover, fly at very low altitudes, rotate in the air, and move backwards or sideways. Many UAS multirotor style platforms are named after the number of rotors they contain. A prefix of quad (4), hexa (6), or octa (8) is followed by copter in order to specify the entire system. Multirotor platforms are well suited for providing nadir and oblique sensor positions, or situations that require vertical takeoff. Many larger copter platforms have the ability for the sensors to be field interchanged via a 'hot foot' connection.

Figure 2: Trimble UX5 - fixed wing

Figure 3: DJI Matrice 100 – quadcopter

Chapter 2

2.0 UAS Sensors

The crucial components within a UAS are the remote sensing devices, as they may directly affect the platforms versatility and navigation. UAS platforms typically have the ability to be solely controlled by the pilot, or flown with the aid of autonomous applications. Recent software development has allowed for preflight planning and flight management systems that provide a careful and beneficial flight design. These typically contain trajectory (waypoints, speed, altitude, etc.) and a flexible real-time mission management capacity (sensor configuration, triggering events, flying directions, etc.) in order to achieve productive and safe missions (Mayr, 2011b). Various remote sensing devices may require a unique application to control data acquisition and UAS piloting. Colonia and Molina (2014) stated that remote sensing is a collection of data while using visible-band/near infrared, multi/hyperspectral cameras, thermal imaging, or light detection and ranging (LiDAR). Red-Green-Blue (RGB) also known as visible band cameras are the most standard remote sensing device mounted on UAS. When the primary sensor is not an RGB camera, a secondary visual positioning system may be needed to assist in UAS guidance.

2.1 PhoDAR & Visible Band (RGB)

Photo detection and ranging (PhoDAR) is a combination of 'photography' and 'LiDAR' techniques (http://www.spar3d.com/news/software/phodar-vs-lidar-new-technology-giant-killer/), and is often referred to as structure from motion (hereafter referred to as the SfM).

SfM follows principles of photogrammetry, and uses software that creates 3D point clouds by processing high-resolution imagery. In a way, it could be said that photogrammetry and computer vision had to join forces to accurately and automatically process UAS-sourced images (Colonia, Molina 2014). Photogrammetric software such as Agisoft Photoscan, Pix4D, UAS Master, and Visual SFM have adopted new principles in order to be able to reconstruct images and create 3D point clouds and surface models. The key to the accuracy and success of SfM are images with high forward and side overlap percentages. Software applications stitch overlapped photos by matching known objects to generate 3D point clouds, surface models, terrain models, mosaics, and orthophotos. SfM point clouds are analogous to the first return data of aerial LiDAR. SfM generates a point derived by each pixel within the photos, and, therefore, the point density directly reflects the spatial resolution of the collected photos. SfM has adopted and improved upon traditional stereo-photogrammetry principles. The quality of the data depends on the type of equipment and sensor used; for example, consumer versus professional grade cameras. Consumer level RGB cameras include those with fisheye or rectilinear lenses with small focal lengths and large field of views (FOV's). Professional cameras with nearly flat lenses, narrowed FOVs and larger focal lengths are able to capture data with minimal distortion. Figure 4 and Table 1 describe three unique RGB sensors and offer specifications for each.

Figure 4: RGB sensors – GoPro Hero 3 (left), DJI Phantom 4 pro (center), DJI ZX5 (right)

Table 1: RGB sensor example specifications

RGB Sensor	GoPro Hero 3	DJI Phantom 4 Pro	DJI Zenmuse X5
Lens	Fisheye	Rectilinear	Rectilinear
~ Focal Length	2.98	3.61	15
Field of View (FOV)	-	84	72
Still Photo Resolution (megapixels)	12	20	20.8
Video Resolution	1080p	4K	5.2K

Consumer UAS's include multirotor platforms similar to the DJI Phantoms, wherein the acquisition cost is below $1600 and the RGB camera cannot be field interchanged with another sensor. The DJI Phantom 4 Pro sensor is built with a multi axis gimble that enables exact sensor positions when mounted on the Phantom 4 series. With proper mounting the

GoPro Hero 3 camera is able to be placed on either a fixed wing or copter style UAS, but captures highly distorted images due to the fisheye lens. The DJI Zenmuse X5 captures the least distorted images of the three sensors shown as its size is nearly four times bigger than either of the other two, and requires a professional grade UAS platform. Professional-grade UAS platforms cost on average more than $3K, and can come with field interchangeable sensor capabilities, multiple battery housing, as well as improved global position system (GPS) equipment. The Zenmuse X5 is shown in Figure 4 with the 'hotfoot' attachment on the gimble, that allows the sensor to be field interchanged.

2.2 LiDAR

The Velodyne LiDAR Puck is a good example of the future of UAS airborne LiDAR. According to the Velodyne system, it is "the smallest, newest, and most advanced product in Velodyne's 3D LiDAR product range". This Puck comes at a cost of approximately $8K, which does not include the hardware mount, GPS, internal measuring unit (IMU), and UAS platform. Phoenix LiDAR Systems is an example of a company who is implementing sensors by Velodyne onto UAS platforms. As this is still considered emerging technology there is not an exact price tag on complete LiDAR package platforms. A ready to fly LiDAR package may initially cost around $100k, but current UAS trends show that after future development the price will probably drop exponentially. The Velodyne Puck specifications when mounted on the Scout platform by Phoenix LiDAR Systems are described in Figure 5. Figure 5 & 6 shows the Scout system sensor in detail, as well as it mounted underneath the DJI M600

hexacopter. Note the Puck sensor is only the black object mounted on the front of the cube, together they create the Scout sensor. The Scout sensor can feature the ability to transmit real time point cloud data via 4G or long range Wi-Fi. As this entire UAS LiDAR system may entail a price tag that is not quite feasible for everyone, PhoDAR is a suitable alternative that is able to produce data of similar accuracies but at much lower costs.

- *Absolute Accuracy:*
  55 mm RMSE @ 50 m Range
- *PP Altitude Heading RMS Error:*
  0.019 / 0.074° IMU options
- *Weight:*
  1.6 kg / 3.5 lb
- *Overall Dimensions:*
  160 * 116 * 116 mm
- *Laser Range:*
  80 m @ 60%
- *Scan Rate:*
  300k shots/s, up to 2 returns

Figure 5: Scout package (left), DJI M600 & Scout package (center), Sensor info (right)

2.3 Infrared (Thermal)

Another leading vendor in UAS remote sensors is FLIR (forward looking infrared). FLIR developed a series of lightweight infrared (IR) cameras that capture rapid and reliable aerial thermal imaging. Data captured in each photo contains relatively accurate temperature measurements that are ideal for analytics and telemetry. Of the two UAS applicable IR sensors offered by FLIR, each pertains to various needs as the lower end camera is priced around $6K, with the higher end being around $10K. Further information is explained in Table 2, followed by the Zenmuse Xt (ZXt) IR sensor in Figure 6. The ZXt is able to be field

interchanged due to the hotfoot system that DJI manufactures on most of their professional

platforms and sensors.

Table 2: DJI ZXt resolutions & specifications

Thermal Imager	Uncooled VOx Microbolometer	
FPA/Digital Video Display Formats	640 × 512	336 × 256
Pixel Pitch	17 μm	
Full Frame Rates	30 Hz (NTSC) 25 Hz (PAL)	
Exportable Frame Rates	<9Hz *	
Sensitivity (NEdT)	<50 mK at f/1.0	
Photo Formats	JPEG (8 bit) / TIFF (14 bit)	
Video Format	MP4	
Digital Zoom	2x, 4x, 8x	2x, 4x
Lens Options	7.5mm, 9mm, 13mm, 19mm	6.8mm, 9mm, 13mm, 19mm

Figure 6: DJI Zenmuse Xt

2.4 Multispectral

Multispectral sensors are also on the rise with professional level UAS's. For example, the

MicaSense RedEdge collects five discrete, narrow bands (blue, green, red, red edge and near-

infrared) using global electronic shutters into distortion free 12-bit uncompressed Tiff files.

The result is claimed to be of radiometric data quality equivalent to trusted multispectral

satellite systems. With the appropriate hardware, this sensor is able to be mounted

underneath both fixed wing or copter style UAS's. Trimble offers the ability to mount the

MicaSense RedEdge sensor underneath their fixed wing UX5 platform (Figure 2). The

product is described by Trimble as having the ability to calibrate reflectance by "acquiring

pre- and post- flight images of a white calibration panel, for which Trimble Access Aerial

Imaging offers an easy and integrated procedure. Additionally, the user has the option to

connect a Downwelling Light Sensor offered by MicaSense to enable continuous ambient

light corrections. The availability of five bands combined with a sound radiometric

calibration enables the user to calculate many tailored vegetation indices for customized

applications" (http://uas.trimble.com/ux5-multispectral). As previously mentioned, all sensor

prices change in correlation to adjacent technology, but current prices for the RedEdge

Camera sensor is around $4500, and displayed in Figure 7. Multispectral data could be

processed within SfM programs and used to determine plant health monitoring, invasive

weed mapping, and weather damage assessment for vast areas.

Figure 7: RedEdge multispectral camera system

Chapter 3

3.0 SfM Techniques for Estimating the Volume of Wood Chips

Volume estimates play a key role in determining the amount of material to be excavated or

inventoried in both environmental and civil applications. The process with which these

volumes are estimated has traditionally consisted of using standard ground-based surveying

techniques. The accuracy of volumetric estimates using traditional methods is resource-

intensive and often limited by project timelines, equipment, and available funds. The

objective of this study is to examine the use of a consumer grade DJI Phantom 3 Professional

quadcopter equipped with an RGB camera for estimating wood chip volume. We collected

UAS photos from multiple sensor positions and then analyzed them using various SfM

programs. From this, we outline a workflow for generating reliable estimates of wood chip

volume.

3.1 UAS Logistics

This study examined the use of a consumer grade DJI Phantom 3 Professional quadcopter for

photo acquisition of chip volume. Although titled as 'Professional' the consumer grade UAS

is equipped with a non-field interchangeable Sony Exmor RGB 12.4 mega-pixel camera with

a 94° field of view (Figure 8). The focal length of this camera is 2.8 mm with a photo ISO of

100 – 1600. Shutter speeds can be set from 8 seconds to 1/8000 of a second. The image size

is 4000 x 3000 pixels, with multiple file formats such as JPEG, TIFF, and DNG. The DJI

Phantom 3 Pro has an integrated camera and records the spatial coordinates of each photo

automatically in the exchangeable image file format (EXIF). The average viable flying time

per battery is around 18 minutes, with a horizontal range limited by FAA line of sight

regulations and a maximum legal altitude of 400 feet above ground level (AGL). The

autonomous flight Map Pilot application by Maps Made Easy was used to capture nadir

images. The Map Pilot application is one of the few that will allow for specific user

customization regarding image overlap, battery management, photo capture, flight speed, and

multi-battery missions. The Phantom 3 Pro can fly over approximately 100 acres at 400ft

AGL using medium flight line overlap (~ 80% front, 70% side).

Figure 8: DJI Phantom 3 Professional quadcopter and remote

3.2 Study Area

The wood chip pile examined in this study is located on an ARAUCO (a private enterprise)

medium density fiberboard (MDF) plant in Moncure, North Carolina (Figure 9). Transfer

trucks arrive at the plant daily to empty their more than 25 tons of cargo (both hardwood and

softwood chips) for refinement into the MDF board. Chips are unloaded via a hydraulic lift,

and transported using an overhead conveyor belt into an appropriate storage bay for

categorization. At this plant, there are four bays for the separation of hardwood and softwood

chips. The volume of chips that enter the facility at the MDF plant is correlated with current

and future production of MDF products. An accurate estimate of the chip volume at the start

of each month allows ARAUCO to calculate the existing inventory and make accurate

manufacturing decisions, including those related to personnel, resources, and profitability.

Current survey methods rely upon third party ground surveyors. Surveyors gather data on the

chip pile at defined intervals, using a GPS and volumetric surveying equipment to recreate

the pile in computer software for estimating the pile volume. Typically, it takes ground

surveyors more than an hour to collect the needed data, and another hour to process the

measurements digitally to estimate a final volume (Figure 14). However, since the ground

surveyors are contract employees, the exact time and cost for the ground survey and

estimation of wood chip volume was not requested.

Figure 9: Study site with wood chip pile and hydraulic lift station at ARAUCO MDF plant in

Moncure, NC

3.3 Photo Acquisition

We collected UAS data once in the months of August and September 2016. Image
acquisition occurred immediately after the ground surveyors finished their data collection (~
8:30 am), to ensure consistency in the amount of wood chips. We did not acquire UAS data
at the same time as the ground surveys, in order to eliminate any possibility of bias in
inventory methods. The UAS was controlled from two main positions that kept the pilot and
visual observer out of the way of transfer trucks and moving equipment (Figure 10). Because
the sun was still rising at this time in the morning, the western side of the wood chip pile
experienced shadow effects during the second survey. Figure 11 shows the area of the chip
pile that was affected by shadows from the low sun angle in September. The inventory day in
August was slightly overcast, and the sun was not visible, resulting in imagery without
shadowing effects.

Figure 10: Mosaic generated via Agisoft of the study site, with an overlay of UAS pilot
positions (star) and equipment traffic areas (red line)

Figure 11: Westward shadow effect on the wood chip pile

Prior to each survey, we required an average setup time of less than five minutes to visually inspect the aircraft, perform a hardware check on the DJI system, calibrate the compass, and designate the GPS return to home point location (within the DJI Go application). After initial setup, the next step was to acquire photos using the Map Pilot application by Maps Made Easy. This autonomous flight software was used to generate a specific flight plan for the August and September surveys, in order to have unique nadir capture locations. The percentage of overlap and the flying altitude were consistently 80% and 130 feet AGL, respectively. At this altitude, there were no physical obstructions, and the resulting ground surface resolution was approximately 0.70 inches. Users can customize the Map Pilot application on an iOS tablet or smart phone, with or without the aid of cellular service or Wi-Fi. Currently, the Map Pilot app is only available through Apple Inc. products; therefore, we used the iPad mini tablet for visualizing real time video during UAS operations. In this case,

we used a smart phone with a personal hot spot, which enabled background satellite imaging to aid in flight line creation on the iPad mini. The percent overlap in nadir photography is critical to matching pixel values, and greater accuracy is possible from a higher percentage of overlap.

We used the autonomous flight software by Maps Made Easy to capture photos in August and September from the nadir position. The DJI Go application was operated to acquire photos of approximately 45-degree oblique's in September (Figure 12). The DJI Go flight application was operated in real time, with the UAS pilot controlling photo capture, platform altitude, and sensor angle. Oblique's were acquired from all sides of the chip pile, at various percentages of overlap, since there is no way to control overlap in the DJI Go application. A 60% side lap in oblique photos was desired, as there were additional photos to add detail in areas the nadir sensor could not capture. Flying altitudes ranged from 0 to 100 feet AGL for capturing the oblique imagery. Total photo acquisition time from setup to breakdown of the DJI Phantom was approximately 20 minutes for each survey.

Area:	2.14 acres
Distance:	0.85 km
Max Speed:	9.0 mph
Duration:	4 minutes 7 seconds
Batteries:	1
Imagery:	57
Points:	Free
Storage:	0.28 GB
Altitude:	131 feet
Resolution:	0.7 inches/pixel
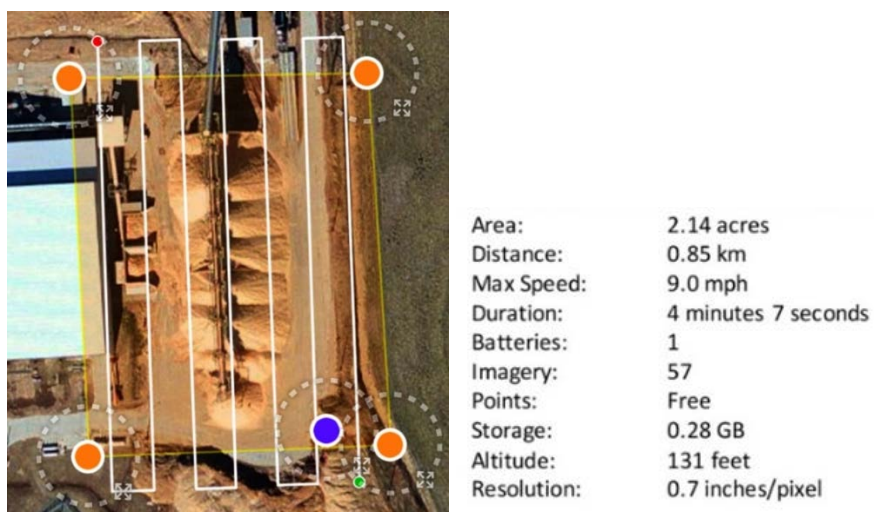
Figure 12: Map Pilot app flight plan and UAS flight logistics
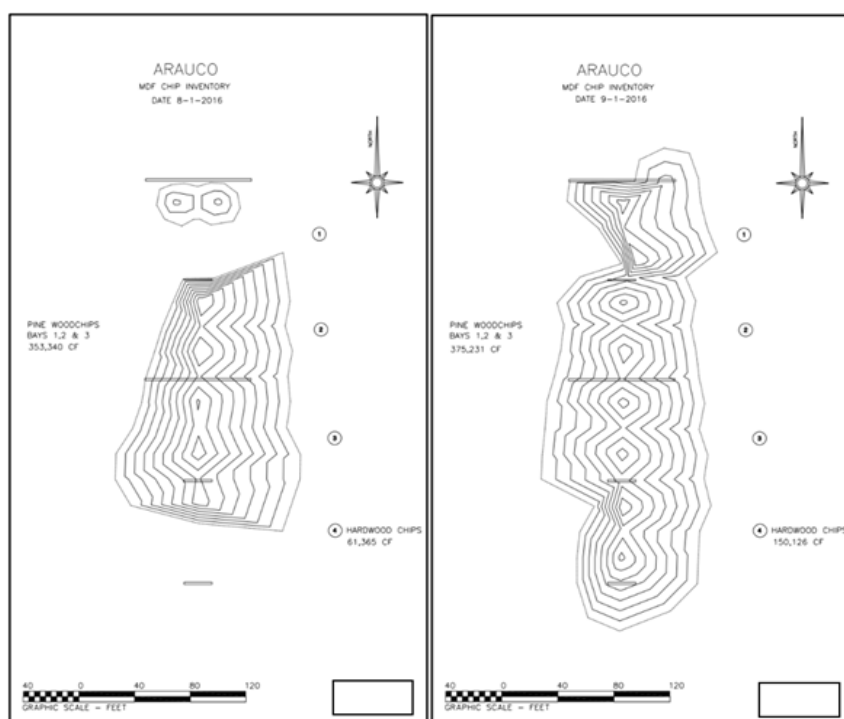
Figure 13: Wood chip pile topo model produced by the ground survey crew for: (left)

August, and (right) September

3.4 UAS Imagery Processing

We analyzed each dataset from the surveys using three different SfM programs: (1) Agisoft

Photoscan Professional Edition, (2) Pix4D Mapper Pro, and (3) Maps Made Easy (Table 3).

Agisoft and Pix4D are licensed desktop programs. They require users to upload, process, and

edit the 3D point cloud on their own computer. Pix4D also permits license holders to use

online image processing, but we did not investigate that option in this study. The Maps Made

Easy online image processor is a 'pay as you go' service that allows the user to specify which

images to upload, and then 'cloud' processing begins.

Table 3: SfM program costs

	Cost per unit license		
	Agisoft Photoscan Pro	Pix4D Mapper Pro	Maps Made Easy
Professional	$3499.00	$3500.00* to $8700.00	$/photo$^\pm$
Student	$549.00	$1990.00	-

*Desktop yearly license $^\pm$Web license

We preprocessed data prior to volume estimation using Agisoft and Pix4D to analyze the

correct points within each dense point cloud. For example, we masked the conveyor belt out

of the 3D point clouds for accurately estimating the chip volume using nadir and oblique

photos (Figure 14). Without removing the conveyor belt, the void area below the conveyor

belt would be included in the volume calculations. We estimated wood chip volumes with the

conveyor belt, using nadir photos for August and September surveys, and used nadir and oblique photos for the September survey. While estimating wood chip volume with the conveyor belt does not allow for the comparison of volumes between the UAS and ground surveyor, it helps to compare the performance of each SfM program. We also estimated wood chip volume without the conveyor belt to compare estimates generated from SfM programs (i.e., Agisoft Photoscan Pro and Pix4D Mapper Pro) and ground-surveyed measurements. Maps Made Easy does not allow customization of the point cloud, and, therefore, we did not estimate only the wood chip pile volume. We repeated the entire process five times with each method to eliminate biased results from each calculation. The average volume and standard error of resulting measurements were used for each method.

Figure 14: Three-dimensional point cloud of wood chip pile 1.1 (a) with conveyor belt, and (b) without conveyor belt

Figure 15: A general structure from motion workflow

Agisoft Photoscan Professional Edition has a simple graphic user interface (GUI) that allows users to select each step and the associated parameters. The workflow is quite simple, and can be batch processed after the initial setup. The final step involves exporting the desired results to the correct file directory. Within Agisoft we used high, medium, low, and the lowest quality parameters to determine the best setting for creating the digital surface model (DSM). The medium quality DSM produced the most accurate representation of the chip pile surfaces in Agisoft (Figure 10). The high-quality processing required a substantial time to stitch points that were considered noisy or above the reference plane. The low and lowest settings appeared to provide incorrect estimates. We also selected medium quality parameters for creating the DSM within Pix4D.

The Pix4D Mapper Pro comes with a GUI, and requires three main processing steps. Steps can be generated individually or batch processed together if selected. The initial phase includes the image capture locations overlaid on a satellite imagery, which is helpful for displaying where the dataset originated and to check for photo inconsistencies. Pix4D and Agisoft allow users to customize the SfM parameters to generate a point cloud that contains the highest accuracy possible. Maps Made Easy application provides systematic instructions on its webpage that require no prior image analysis experience, as there is little customization

of processing parameters. Once photos are uploaded and export parameters are selected, an

email is sent to the user with the suggested time of completion, and the user is again notified

via email when the process is completed.
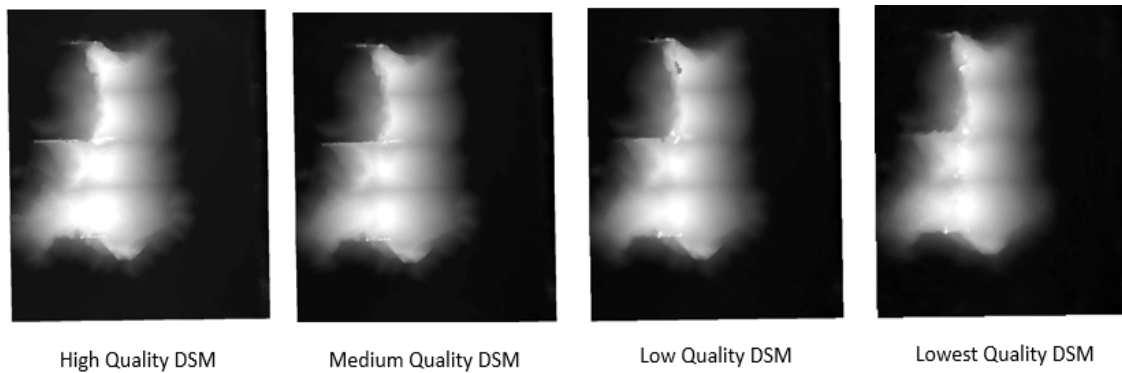
Figure 16: Agisoft dense point cloud quality setting comparison for DSM generation

3.5 Results

Volume estimates varied across the applied SfM programs. The Pix4D Mapper Pro program

produced the smallest standard errors in estimating wood chip volume, both with and without

the conveyor belt, using nadir photos for August and September UAS surveys (128 and 26

m^3; 83 and 14 m^3, respectively) (Table 4). Maps Made Easy produced slightly higher volume

estimates with the conveyor belt for August and September (3.5% and 2%, respectively),

compared to the Pix4D Mapper Pro program, but at the cost of the highest standard errors

(380 and 523 m^3), whereas Agisoft produced volume estimates approximately 19% higher

(Table 4). The three SfM programs produced the largest volume estimates and standard

errors using a combination of nadir and oblique photos for September (Table 5). These

volume estimates were far from those of ground-based survey methods. When we removed

the conveyor belt from the 3D point cloud, we observed volume estimates similar to those of

the ground survey, while standard errors were the lowest (Table 6). The Pix4D Mapper Pro

program produced the lowest standard error (14 m^3), followed by the Agisoft Photoscan Pro

programs (27 m^3 without the conveyor belt). Volume estimates from these two SfM

programs were 8 to 12% lower compared to the ground survey (Table 6). We found that the

standard error of volume estimates decreased as the number of photos used in the image

processing increased. The SfM programs that produced the lowest average standard error

used the highest number of images, such as the Pix4D Mapper Pro program.

Table 4: Estimates of wood chip pile volume (m^3) with conveyor belt from nadir photos,
using three Structure for Motion programs for August and September

	August		September	
	Volume (m^3)	Standard error	Volume (m^3)	Standard error
Agisoft Photoscan Pro	15720.7	147.8	20128.7	57.6
Pix4D Mapper Pro	13252.8	128.1	19468.8	25.7
Maps Made Easy	13708.1	380.0	19859.5	522.5

Table 5: Estimates of wood chip pile volume (m3) with conveyor belt from nadir photos for September, using three Structure for Motion programs

	September	
	Volume (m^3)	Standard error
Agisoft Photoscan Pro	20362.6	113.4
Pix4D Mapper Pro	19459.4	192.6
Maps Made Easy	20750.4	668.3

Table 6: Estimates of wood chip pile volume (m^3) without conveyor belt from nadir and oblique photos for August and September, using the Agisoft Photoscan Pro and Pix4D Mapper Pro

	August		September	
	Volume (m^3)	Standard error	Volume (m^3)	Standard error
Ground survey	11743.10	-	14876.50	-
Agisoft Photoscan Pro	10358.70	193.80	16626.80	27.40
Pix4D Mapper Pro	10769.00	83.00	16231.50	13.80
Maps Made Easy*	-	-	-	-

* Preprocessing, such as removal of unwanted 3D points, is not available in this program

3.6 Discussion

The UAS allowed for seamless data collection amidst heavy equipment operating around the chip pile. Since there is minimal site disturbance through the UAS data collection procedure, UAS can be used on a regular basis for monitoring wood chip pile volumes in order to update inventory. The Pix4D Mapper Pro program outperformed the other two SfM programs, with the lowest standard error and volume estimates, similar to those of the ground survey. The Maps Made Easy application is much simpler if the user does not have prior SfM knowledge, or insufficient computing hardware. It is important to keep in mind that the data collected via ground survey is also only an estimation, and could be biased. Besides generating and saving multiple volumes at once, SfM programs provide high-resolution mosaics and 3D interactive models that could be used for additional purposes. Byproducts such as the mosaic generated by SfM techniques when estimating volumes may help for inspecting conveyor belts and auditing infrastructure.

Photo acquisition should follow procedure to minimize the shadow effect. While shadows in wood chip pile photos did not affect the quality of the DSM, they did affect the RGB values of photos. UAS pilots should account for the clarity of the atmosphere, sun angle, wind speed, and changes in camera exposure to acquire usable photos in a timely manner. If these parameters are not addressed, the photos may be blurry and out of focus and unable to be stitched together. We successfully imported imagery collected by the DJI Phantom 3 Pro into multiple SfM programs to generate and view high-resolution 3D point clouds and to reference spatially. SfM allows for the mapping of areas at resolutions that were previously

not possible, and is a valuable aid to natural resources. However, each program has its pros and cons, and should be used accordingly to maximize the objectives of a project.

The Agisoft Photoscan application performs photogrammetric processing of digital images and generates 3D spatial data. This provides an easy and fairly rapid calculation of volumes, but it is difficult to get exact results for large areas with specific boundaries. Tools that are used for volume delineation do not allow the user to select exact pixel locations, and can cause confusion if irregular or vast areas are to be calculated. The general workflow is quite simple, and photos can be batch processed after a quick setup. Generated mosaics are of high quality, with uniform color distribution across the entire project area.

The Pix4D Mapper application uses three main processing steps that generate a simple workflow. It provides accurate clipping and volume extraction methods that allow the user to save and view multiple volume measurements at once. Another appealing feature that Pix4D offers is the ability to save the entire workflow as a template; therefore, it can be easily loaded for a new project. This decreases the possibility of error when selecting the SfM parameters, and allows for time efficiency with repeated image processing.

The Maps Made Easy application operates through a system that requires the user to pay for the image processing, using a point scale associated with the amount and resolution quality of the photos. There is a direct correlation with resolution and suggested computing power; therefore, Maps Made Easy accounts for this input variable. The current version permits projects that are less than 250 points to be processed free of cost, to allow users to test the system and run sample areas before processing large datasets. Each chip pile dataset did not

exceed 250 points, and was able to be processed without cost. Maps Made Easy is the easiest method of processing, as it requires very little user input and knowledge. Volume areas are delineated through a 2D interactive window, where the user selects volume boundaries via the generated mosaic. However, users do not have the ability to edit the point cloud, making volume calculations include all space below overhead features. Project deliverables are easily accessible to view and download in 2D and 3D formats.

SfM programs are able to account for minimal changes in topography. Desktop-based programs, such as Agisoft and Pix4D, are optimal for acquiring and preprocessing data that includes removal of 3D points of unwanted overhead features that may obstruct the calculation of volumes. If the area surveyed does not have any overhead features, a program such as Maps Made Easy is another outlet at a low cost of operation. The front-end loader that is visible in the eastern side of the mosaic (Figure 12) was able to operate continually when the UAS survey was being conducted, while this was not the case with the ground survey. Therefore, the UAS pilot was able to conduct inventory from a safe distance away from moving equipment compared to ground surveys, therefore decreasing the possibility of an accident occurring during the UAS survey. The ability to provide a standard error, specifically tailored to each dataset, with UAS measurements can offer additional data regarding the volume estimation, in comparison with a typical ground survey method.

3.7 Conclusion

This study demonstrates that post-processing of UAS imagery using multiple software approaches for estimating wood-chip pile volume is repeatable, and comparable to estimates produced by ground survey. The point cloud generated through only nadir photos had a larger standard error when compared to that of the images gathered in nadir and oblique positions. Oblique photos captured the vertical texture of the pile in a way that the photos provided by the nadir sensor was unable to. Photos captured with a tilted sensor acquired at various altitudes and angles mapped different aspects and surfaces that were unseen in nadir photography (especially underneath the conveyor belt). We found that the standard error of the chip pile volume decreases as the number of photos used in the image processing increases. The dataset with the highest number of images had the lowest average standard error. A direct comparison of known wood chip volumes to those estimated by SfM programs is needed to improve the accuracy of volume estimates. This will inform us of the bounds and errors of each used program, and their ability to successfully generate an accurate 3D point cloud. Adding survey GCP to tie the models to true geographic coordinates may increase the accuracy of estimated volumes, and should be taken into consideration.

Chapter 4

4.0 Applications of UAS technology to monitor Atlantic white-cedar (AWC) on Hofmann
Forest, North Carolina

Every field forester or environmentalist that has worked in dense vegetation and low lying
areas understands that field work in remote areas can be difficult and time consuming.
Atlantic white cedar (*Chamaecyparis thyoides)* (AWC) is native to the Atlantic coast of
North America and considered an obligate wetland species. "Atlantic white cedar is one of
only six species in this genus. Only three of the six are native to the continent, and two of
them are west coast species. This leaves Atlantic white cedar as the only representative in the
East, where it occurs in a narrow band along the Atlantic coast. Atlantic white cedar is an
evergreen with scaly leaves that occur in a flat fern-like appearance. This species usually
grows in very dense, solid stands, and has small rounded cones" (USDA 2002). The tree
tapers to a point, giving it a cone like shape. AWC thrives in hydric soils and often has to
compete with low lying ground and mid story vegetation. Dense stands in low, wet areas,
including freshwater marshes, swamps, river banks and wet woods can contain a diverse
ecological site that hosts many animals and plant species that are often found on endangered
and protected lists. "The habitat of this species is very limited, and increasingly rare due to
coastal development" (USDA 2002). AWC seeds are winged and very light, and may be
carried long distances by strong winds. The wood is considered a commercially important
product due to the durability, rot- and decay-resistant properties.

Figure 17: Native Range of Atlantic white cedar (Chesapeake Bay Program 2016)

For any timber to be a viable forest product, it typically has to be managed with silviculture prescriptions, or at least monitored. AWC is still a desired forest product, but the management of this species on the Atlantic coast is dissipating. For this reason, there is a need to monitor current and future AWC stands in a means that is efficient, accurate, and inexpensive. The objective of this study is to count young AWC regeneration, map its spatial spread, and estimate AWC tree heights using inexpensively acquired UAS aerial imagery, publicly available LIDAR, and GIS software to maximize data collection efficiency while minimizing cost and time.

4.1 Site Location

Hofmann Forest (HF) is an 79,000 acre forest centered on a pocosin having some of the oldest planted Atlantic white cedar [*Chamaecyparis thyoides* (L.) B.S.P.] (AWC) in coastal North Carolina. The earliest AWC plantations in HF were established in 1965 as several acres in species trials at the intersection of Quaker Bridge and Pocosin roads near the center of the pocosin. The 1965 planted AWC was never fostered in any way, but was able to slowly reproduce immediately adjacent to the original planting. The dense shrubby nature of the natural pocosin vegetation precluded significant spread of AWC in the area. In 2010, an 80 acre block across the road from the original 1965 planting (hereafter referred to as 'Parent' trees) was cleared and site prepared to plant longleaf pine. Normal longleaf pine site preparation involves herbicide followed by strip-shearing and bedding. Immediately after exposing the bare organic soil in the longleaf block, the Parent trees began to release seeds that would take a thriving foothold in this area. There is no other potential nearby AWC seed source, so this is an excellent place to examine the natural seeding pattern and spread of AWC after site disturbance.

Figure 18: Hofmann Forest boundary

Figure 19: UAS oblique view of study area

4.2 Photo acquisition

Images were acquired with a DJI Phantom 3 Professional quadcopter equipped with a Sony Exmor 12.4 megapixel camera in the fall of 2015. Five 3ft by 3ft ground control panels were set along the gravel road at equally spaced intervals. A Trimble GeoXt 2008 unit with +/- meter accuracy was used to gather a single location of the center of the GCP's. No ground control panels were placed within the timber stand as the vegetation was too thick to navigate.

Multiple flight plans were created in order to determine the optimal flying altitude to inventory the AWC stand. Parameters taken into consideration were number of batteries used in each mission, total photos acquired, and ground surface distance (GSD) resolution. Approximate altitudes of 75, 130, 160, and 200ft above ground level (AGL) with 80 percent image overlap were considered.

In order to determine flight boundary areas, prior site reconnaissance via manual UAS flight via the DJI Go application was required in order to ensure all AWC trees in the project area would be mapped. The Drones Made Easy Map Pilot application allowed us to quickly and efficiently create flight plans while at the study site on an iOS tablet. Thanks to the waypoint navigation provided by the Map Pilot app, the UAS can be operated fully autonomous including auto start and auto landing. The flight route is programmed using a graphical interface with satellite imagery, followed by a wireless upload to the UAS. Within the application appropriate actions to take on each flight line are designed, including photo shutter rate, photo orientation, trigger activation, and battery management. As the altitude is

measured based off of the takeoff location, complete site checks were made to ensure there were no above ground obstacles that would interfere with the flight.

Each flight was planned in the Map Pilot app, to determine if the flight was feasible for the project area. The flying altitude of 75ft AGL required the most intense flight plan, requiring the copter to fly over two hours. Further information regarding each flight plan can be seen in Table 7. An additional flight was made at 200ft AGL to cover the entire study area, in order to identify any of the surrounding Parent trees. Figure 20 displays a real-time screenshot of the Map Pilot app during image acquisition of project area. The red triangle is the copter location, while gray dots represent previous photo locations on flight lines.

Table 7: Map Pilot application flight characteristics

Flight Number	0	1	2	3
~ Altitude (ft. AGL)	75	130	160	200
Duration (minutes)	135	35	28	20
Batteries	8	3	2	2
Images	2512	715	511	342

Figure 20: Screenshot of the Map Pilot app over AWC project area

4.3 Data Processing

Once photos have been acquired via various flight plans the 3D model building may begin.

Since the photos are already georeferenced the flight plan does not need to be imported into

the SfM program of Agisoft Photoscan Professional Edition. As Table 7 describes, an

increase in flight altitude, lowers the overall image count for the mission. As processing time

is directly correlated to the number of images uploaded into the program, the higher flight

altitude missions took less time to process. Exact processing time varies per computer, as

CPU, GPU, and RAM are optimized heavily. An increase in any of these parameters will

lower the total processing time. Through a series of pre-determined workflows within

Agisoft, we were able to generate and export a mosaic and digital surface model from each

flight without using any GCP's. The outputs generated from flight 1 were determined the

optimal results and used for all further analysis.

The next step was to determine if the ground control would aid in proper orthorectification. After multiple processing trials regarding ground control placement, the GCP's were omitted from processing due to the biased vertical accuracy of the GCP's, and the lack of uniform distribution across the entire stand.

Log ASCII Standard (LAS) files having a resolution of 2 postings per square meter (with as many as 5 returns per posting) were downloaded from the recently created beta website hosting the 2014 LIDAR flown in coastal North Carolina (www.rmp.nc.gov/sdd/). Bare earth points were exported using open source LIDAR software (Fugro Viewer). We were not interested in any other point returns since we were only focused on finding where the trees begin growing (the ground elevation). As the LiDAR data was acquired at a different time than UAS image acquisition, we did not plan to compare timber height estimations between UAS and LiDAR sensors as the trees would have increased in height. The LAS bare ground point cloud was imported into ArcMap to create a raster digital elevation model (DEM). As the DSM from Agisoft was not orthorectified with ground control points, the mosaic was also imported into ArcMap and manually aligned with the LiDAR DEM. This process was able to occur as the elevation of the dirt roads on either side of the timber stand should not have changed since the acquisition of the LiDAR data. Using the raster calculator tool within ArcMap the DEM was subtracted from the DSM to generate a canopy height model (CHM) (Figure 21).
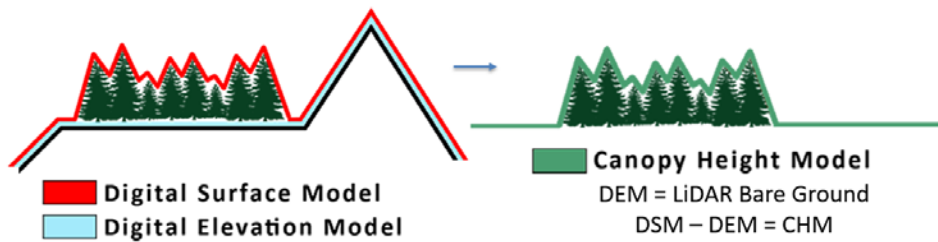
Figure 21: Canopy Height Model (CHM) explained

As the CHM includes all vegetation, the next step required manually locating and marking each AWC tree within ArcMap. This process was completed via visual interpretation of the high-resolution mosaic. All visible AWC trees with the study area were digitized. In order to determine relative heights of mapped AWC trees the raster values from the CHM were extracted at each tree location.

An unsupervised image classification of the generated mosaic was processed through ArcGIS Pro. We decided to break the image into four different classes, hoping the computer could aid in plant identification. We decided to use more of a generic classification since the spectral values between AWC and longleaf pine are very minimal in UAS imagery. Breaking the image into bare earth, conifer, shrub layer, and other categories would allow for a quick vegetation distribution map to be generated with very little effort.

Ground truth measurements of the AWC trees were attempted shortly after the flights were conducted, but due to the extremely dense vegetation and extensive resources required to gather even a reduced sample, it was aborted. The field data that was collected was omitted as it did not represent enough area to be used for regression comparisons.

4.4 Results

Flight 1 was chosen as the optimal source of data as it did not require extensive in air time to acquire photos, and the point cloud & mosaic generated within Agisoft is of high resolution. Although any of the flights with higher altitudes could have been chosen, we found that lowering the flight altitude increased the overall point density. After one hour of digitizing the flight 1 mosaic, we spatially mapped 1,563 AWC trees in the project area through visual interpretation. The mosaic generated from the 200ft AGL flight of the study area was used to digitize 132 Parent trees outside of the project area (Figure 22). Spatial locations were applied to the terminal buds of each tree, as we were trying to identify each tree only once. Buffers were applied to the Parent trees closest to the study area, in order to determine the seedling dispersal distances (Figure 22). Trees per acre (TPA) were calculated by data derived in the six buffer distances.

Since the LiDAR bare ground data (DEM) and the canopy surface (DSM) generated by Agisoft were available, the difference between the two layers could be computed within GIS. This allowed for the generation of a CHM (Figure 23) of the project area. The CHM image contained 5,785,483 pixel values, each containing unique representation of surface model elevations at those locations. By extracting the height value at each AWC location, an average height of 10.5 feet, with a standard deviation of 3 feet was determined. Appendix B shows a clear image of this product and is titled 'Agisoft Canopy Height Model Limited to 8ft AWC Buffer'. Without applying an 8-foot buffer to the AWC locations height values were unable to be visually represented. Negative pixel values in the CHM associated with

drainage ditches along the NW, SW, & SE sides of project area were excluded. When

compared to the mosaic (Figure 23), features such as the ditches, as well as roads on the east

side, are easily recognizable. When examining the road elevations in Figure 23 (CHM) on the

northwest side, one may note how there is an increase in elevation as depicted by the green

symbology. This is due to SfM processing without GCP, as the center of the model is

generated with higher elevations since there were no reference points to tie the model to

correct elevations. Latitude (X) and longitude (Y) wise the model was nearly correct when
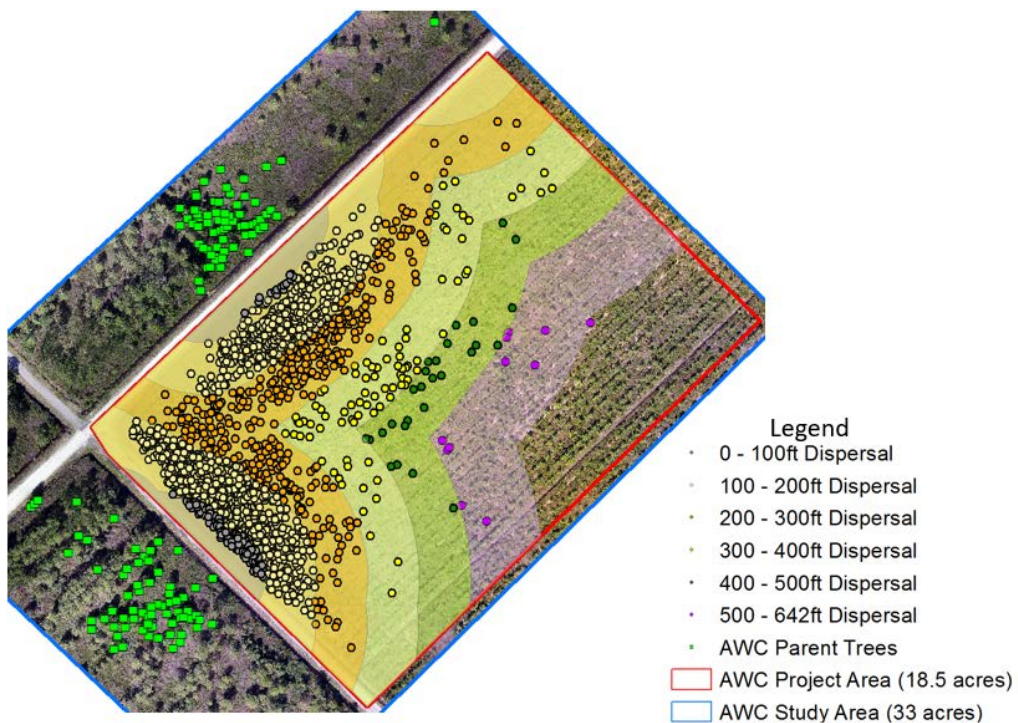
compared to satellite based imagery.

Figure 22: Seed dispersal distances overlaid on high resolution mosaic

Table 8: AWC seed dispersal

	Buffer Width (ft) from Single Parent AWC Tree					
	0 - 100	*101 - 200*	*201 - 300*	*301 - 400*	*401 - 500*	*501 - 642*
AWC Count	116	920	400	89	27	11
Tree's per Acre	400	418	112	28	11	4

The AWC seed dispersal statistics shown in Table 8 demonstrates the magnitude of how thick AWC can regenerate if allocated the proper resources. Within the first 100ft buffer distance, nearly half of the area is covered by gravel road, therefore the total AWC count does not reflect what would be predicted from the adjacent buffers.
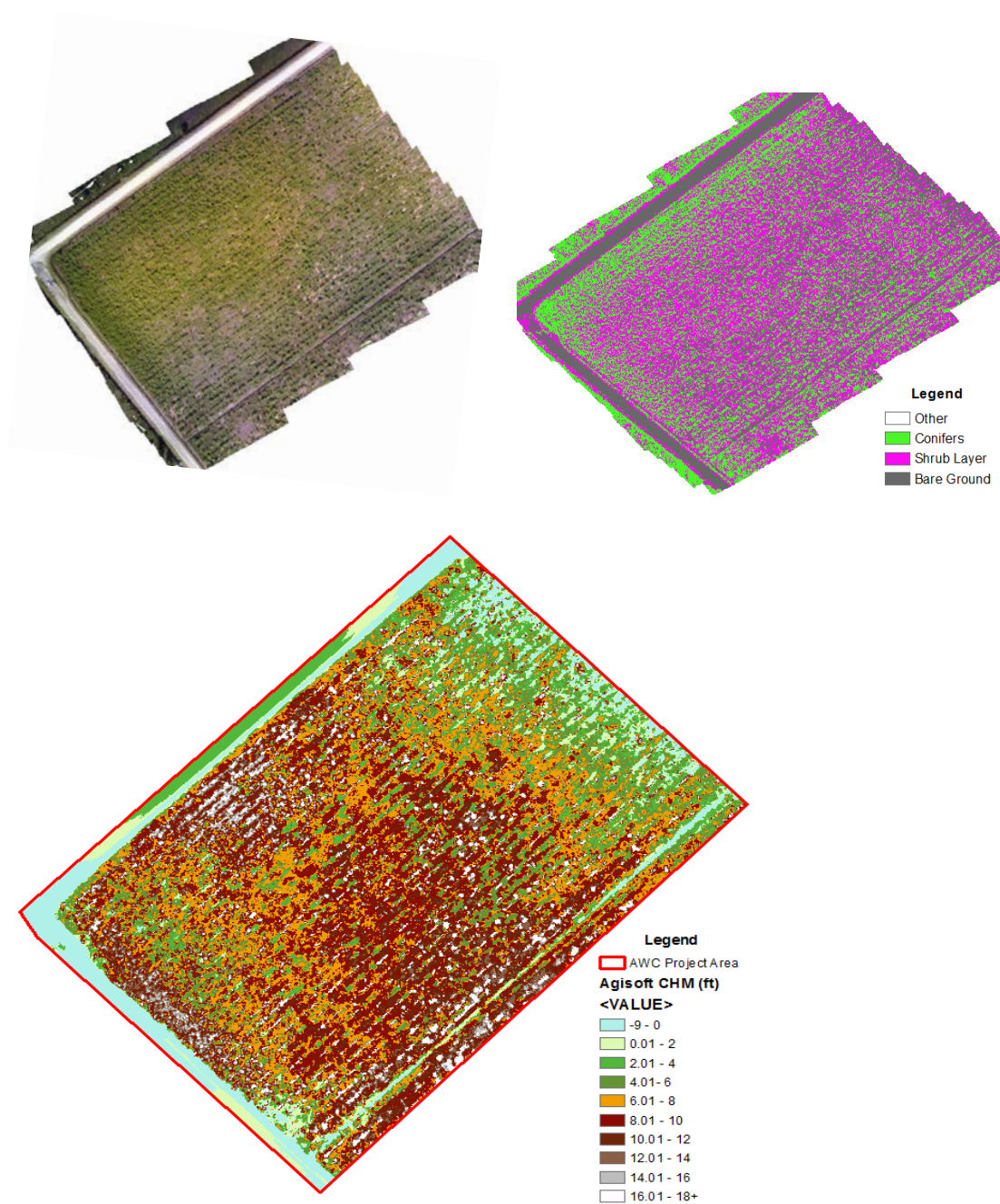
Figure 23: Mosaic (top left), Unsupervised Classification (top right), and CHM (bottom)

derived from Flight 1 data

4.5 Discussion

We feel confident that we were able to spatially locate all of the AWC trees within the study

area that were visible through the mosaic image. Granted any seedlings that were surviving

underneath the canopy were not able to be mapped. These non-dominant trees have a low

likelihood of surviving due to their limited resources, so identifying them may not be of high

concern. Flying the site when most of the vegetation was dormant allowed for the AWC and

other conifer species to be distinguished in the mosaic with unsupervised classification,

rather than a growing season flight when everything would be green.

One problem that was discovered when identifying trees on the edge of the stand near the

ditches, was the likelihood of a single tree having multiple terminal buds. This was originally

discovered during the attempted field surveys. Figure 24 shows how a single tree can

originate from one stump, but have multiple stems that may reach the canopy. This would

decrease the overall AWC count within the study area as a single tree could have been

represented by multiple marked terminal buds.

Figure 24: Multiple AWC stem scenario

Using ArcMap and ArcGIS Pro to determine variation in species across the project area was

successful in providing a generic distribution of conifer species. The mosaic does not provide

a uniform color balance due to shadow effects by clouds and variation in photo color balance

ratios, and would cause an issue if detailed classifications were desired. The furthest mapped

AWC tree was ~ 642 ft. away from the nearest Parent tree. Although this calculation

disregards the possibility of AWC trees within the study area to be a seed source, it does

demonstrate AWC's regeneration pattern. We think that if sufficient time was allocated,

AWC would eventually consume the entire 80-acre block with natural regeneration.

When determining timber heights, the surface model that was generated in Agisoft was used

for raster calculations. We found that this surface model represents terminal buds with more

of a rounded surface, rather than a conical shape when modeling the top point in the point

cloud. Therefore, the very tip of the tree may not have been used in estimating the height

from the DSM. From below, the LiDAR bare ground elevations should be correct, but there

is possibility a variation occurred when aligning the DSM to the DEM. As the examined data

was processed without ground control, the model appeared to have a slight inverse 'bowl'

like shape. Height values in the center were modeled higher in comparison to other values,

while values in the northeast region tapered lower in response to the lack of GCP.

Computational power could impact the ability to map very large areas at high resolution, but

even at a 400 ft. AGL, the DJI Phantom 3 Pro has resolution slightly greater than two inches.

Therefore, mosaics could be generated from flights at the maximum legal altitude in order to

reduce in air time and speed up SfM processing as the total image count is reduced.

4.6 Conclusion

Monitoring AWC in densely vegetated or remote areas can be difficult and time consuming. Using a UAS to spatially locate, map the spread of, and determine heights can be an inexpensive & valuable aid in this species management. UAS imagery acquired at initial planting could be used to develop a bare ground DEM which future DSM's could be compared against to make updated timber stand CHM's without the aid of LiDAR data. If accuracy greater than estimations are required, having survey grade GCP's to develop both the DSM and DEM would be required. Evenly distributed GCP's would also help eliminate the inverse 'bowl' shape. Generating the canopy DSM through point cloud interpretation in another program besides Agisoft could increase accuracy when mapping the terminal buds. Programs that are more robust and customizable at handing these unique types of point clouds could be of aid.

The ¾ inch GSD mosaic derived by UAS photogrammetry with 80% overlap captured at ~130ft altitude provides more than sufficient resolution to identify individual trees. With over 5 million pixels with height information in an 18.5 acre area, enough data was generated to perform relative height estimations. There are many confounding variables that may affect the results of this project that could be improved, yet the overall goal of identifying AWC and estimating timber heights was accomplished. We discovered that even trying to ground truth our own measurements in the dense stand required extensive resources to accomplish, therefore further proving that aerial methods drastically reduce the time to survey a remote site.

Chapter 5

5.0 Other Use Case Scenarios for UAS

Proper stewardship of our natural resources can benefit from the application of new technology and equipment to make informative collection and therefore decision making more efficient. Technology is continually improving and changing within the natural resources field. What we have to do as proper stewards of the environment is learn how to use new equipment and technology in the most beneficial and efficient way possible. This chapter highlights several areas where UAS can be directly incorporated into Forest and Natural Resources Management using various remote sensing devices.

5.1 Prescribed Burn Monitoring

RGB and IR cameras from a UAS can aid in smoke and spot fire identification, as well as instantly be able to check the progress of a burn to ensure complete coverage. This is especially convenient when working with prescribed fires where a UAS is able to quickly fly the entire site and see if there are areas that need re-ignition. RGB and/or IR sensors can be used to check existing fire lines as well as 'black' areas that have already been burnt to ensure the fire is contained. Figure 25 displays an RGB image captured of an area where a small charcoal fire was smoldering in a metal container underneath pine canopy. The fire is nearly impossible to see from a visible light source. At the same altitude, the IR camera is able to easily detect the small fire (marked by the red arrow) depicted in Figure 26, with a black is hot color scale. As the IR photos retain generic heat values regarding each pixel,

computer programs are able to automatically detect the hottest and coldest spots, as seen in

Figure 26. The blue arrow is pointing to the coldest area, corresponding to a metal roof on a

winters day. Figure 27 shows to the same area, but with an IR capture altitude of

approximately 150ft AGL. The symbology in both Figures 26 and 27 display black as hot

temperature values. Notice the clarity of the IR data in Figure 27 since there is less 'noise'

associated with lower capture altitudes.

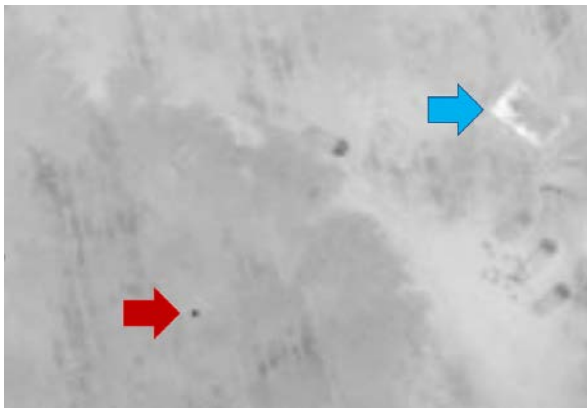Figure 25: RGB ZX5 image at ~ 400ft AGL

Figure 26: IR ZXt image at ~ 400ft AGL

Figure 27: IR ZXt image at ~ 150ft AGL

As photos taken at a lower altitude offer increased temperature data, combining multiple photos with high percentages of overlap through SfM programs is also beneficial. Figure 30 is a unique 3D model that displays the IR values via symbology, of each pixel in a mosaic that was generated in an SfM program. This mosaic is opposite of the previous figures, as heat signatures are displayed in white, while cooler objects are shown in black. Notice in this parking lot some car hoods are white as the engine was still emitting heat!
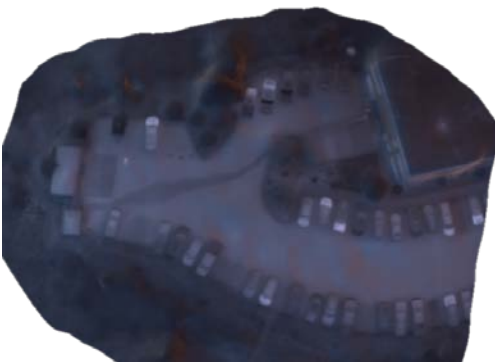

Figure 28: 3D model generated in Pix4D of IR data acquired with ZXt sensor

As the resolution of the IR camera is nowhere near as high as standard cameras, the resulting

3D model does not retain all vertical structures. Taking many photos at high overlap while

flying at a lower altitude allows the heat signatures to be represented at an accuracy greater

than a single photo at higher altitude could accomplish. This IR mosaic could be draped over

an accurate 3D model that was generated via a RGB sensor of higher resolution that may

incorporate GCP's to better depict the site in 3D.

5.2 V-Shear & Bedding Inspection

Applying UAS in the field to check progress of the planting equipment and calculate total

area completed as well as the remaining acres is a great way to decrease time spent with

typical boots on the ground inventory. When a site becomes too wet for the equipment to

continue operation, the forester usually has to walk the tract or rely on the contractor for an

assessment of the remaining acres. By combining UAS, SfM, and GIS technology we are

able to determine the total area left to complete the job (on a per acre basis), therefore the

remaining cost and time to complete the site prep can be calculated. Knowing this

information can allow for better contractor/equipment scheduling to ensure each stand is able

to be reached on time and be done so with minimal time wasted. In order to decrease the

'down time' of a timber tract one can quickly fly each site to see if proper drainage has

occurred before physically walking to each area and noticing something they could have

determined in a quarter of the time via UAS. Figure 31 and 32 are oblique photos that took

minutes to acquire, but shows valuable data according to site drainage and bedding progress.

Figure 29: Site drainage inspection

 Figure 30: Bed inspection

Once the beds have been implemented the distance between the centers of bedded rows can

be calculated from combing overlapping UAS imagery of the site. Typically, bed inspection

is conducted via ground measurements and can be an exhausting and time consuming

process. Using a mosaic of the site generated via an SfM program, we are able to calculate

similar data within GIS programs. Figure 33 describes the flight plan of a 16-acre site, that

took 10 minutes to fly with a DJI Phantom, capturing 150 images at an altitude of

approximately 250ft.

Figure 31: Screen capture of the UAS flight plan in the Map Pilot app.

The resulting site mosaic had a resolution of 1.3 inches per pixel. This high-resolution

mosaic is able to provide relative measurements to check and see if desired bed spacing

requirements are met. Figure 34 displays how a specific size plot can be created so that

various sampling methods can occur within GIS. In Figure 34, the red circle is a plot created

in a random location on the site, the NW to SE directional white lines depict bedded row

centerlines, while the green polygons outline the timber crown shapes. If multiple plots were

established over the entire mosaic, the forester would essentially 'cruise' the stand via a
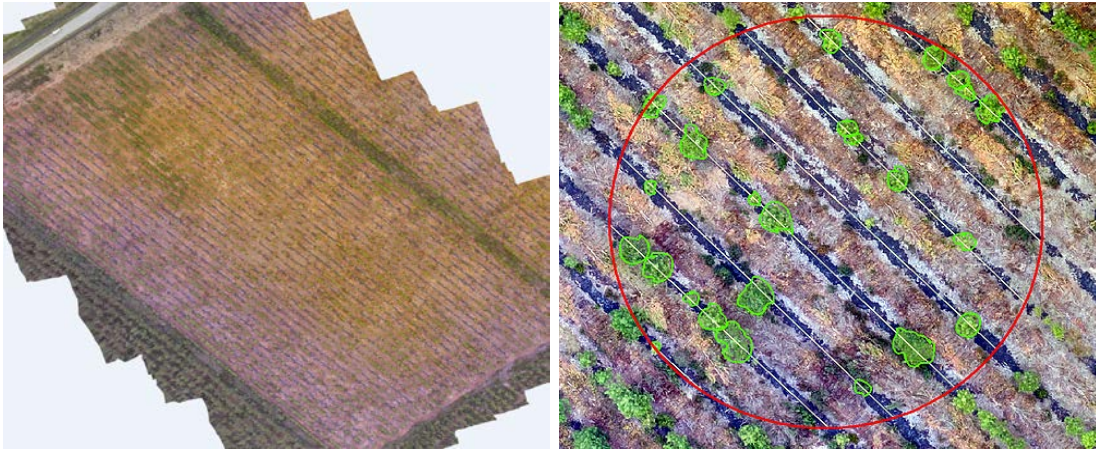
georeferenced mosaic.

Figure 32: (a) Mosaic of site, (b) fixed radius plot sampling within GIS

5.3 Herbicide Inspection

One can inspect a site that has been sprayed for herbicide (prior or post planting) to ensure

proper coverage and application. In order to inspect a site that has received herbicide

application by boots on the ground methods, a forester would have to walk the entire tract or

place multiple plots to ensure the invasive species have been efficiently treated. Via UAS

one is able to efficiently determine if the entire tract received an even treatment, inspect

buffer areas to ensure no herbicide encroachment, calculate mortality of overspray areas (if

any), or view and document areas that need re-application of the same or different herbicide

application.

There is also the ability to predict and delineate specific areas within a stand (compared to

the entire stand) that need a specific fertilizer or herbicide application, therefore decreasing

site prep/management costs and minimizing environmental impact. If the operator has

appropriate certifications there are even UAS platforms equipped with small bladder tanks

that are available to apply herbicide at an estimated rate of 7-10 acres an hour (Figure 35).

Figure 33: AGRAS MG-1

5.4 Harvest Audit

Aerial harvest inspection can ensure each acre is accounted for across the stand. Using a

UAS, foresters can ensure uniform application and spacing of a PCT across the stand prior to

the contract crew leaving the site. Whereas determining this by a field forester on foot would

take a considerable time and expense. Often it can be very difficult to calculate the remaining

area of a thinning operation while on foot, yet from an UAS one can easily determine an

accurate acreage via mosaic interpretation in GIS. A UAS can provide pre-harvest

information at young ages that can lead to increased knowledge of stand productivity in

regards to optimal tree genetics and spacing. Stands that have yet to be pre-commercially

thinned (PCT), drum-chopped, or commercially thinned often are so thick or large it may

take hours to navigate on foot. Knowing if certain management regimes work years prior to

commercial thinning will allow for future stands to be managed with similar characteristics, leading to an overall increased annual production.

During the wet season since loggers are often moving to various tracts searching for dry ground. The result of this process leaves many tracts with un-harvested areas that a forester then has to manually GPS in order to determine the remaining volume and profit. UAS aerial reconnaissance would allow for better allocation of resources.

Figure 34: Oblique UAS view of a thinning operation

A final post thinning audit flight can reveal if any remaining timber were severely scarred or damaged to the point of crown mortality. Additionally, there is the ability to easily track logger progress and offer updated maps on specific areas such as: wet spots, streamside management zones, landing sites, skid trail placement, and boundary lines. Overall uniformity and slash/lap placement can be audited, for easier future site preparation. One is also able to identify any remaining timber that has been cut but left on the ground (Figure 36). This may occur if the site became too wet and timber was missed during skidding to the landing. Being able to quickly determine the number of logs are left leads to a better

estimation of the profit that is remaining on a stand, without having to manually survey the

wet areas on foot. In the mountain region Christmas tree plantations, can be flown prior to

harvesting to easily get a record of the number of trees growing. Post-harvest the site can be

flown via the same flight path and the total number of trees harvested can easily be calculated

when compared to the previous mosaic.

Figure 35: Inventorying harvested logs in a flooded area

5.5 Natural Disaster Inspection

In the instance of a hurricane, tornado, flooding, beetle kill, fire, and wind/ice damage a UAS

is able to safely inspect and determine the total impact. Without having to physically place an

individual under broken canopy or near fast flowing floodwaters allows for a safe approach

and increased knowledge of an impact that may need direct attention.

5.6 Hydrology Management

As referenced before, having an undesired amount of water on a site can not only halt contractor/operator productivity but greatly impact a sites compaction and drainage capability. Stream and ditch management surveillance and focused views on culvert operation during times of high flood waters can allow for an increased knowledge on areas that need improvement. Having the capability of aerially determining where the water is coming from and how to resolve the situation (improved culvert location/size) during times when a forester cannot access the site is very beneficial.

5.7 Mitigation Bank Monitoring & Delineation

UAS imagery can aid in determining species concentration as well as view regenerating species in existing banks. Encroachment of desired or undesired species can be mapped and tracked over any defined interval of time. Image interpretation through supervised or unsupervised classifications can lead to computer based delineation of major plant species. UAS decreases site disturbance nearly one hundred percent since all measurements are gathered from remote sensing. If proper GCP points were established the stream and corridors could be digitized to compare to initial site plans. The ability to efficiently survey every square foot of the site, at an accuracy of a few inches is an irreplaceable tool. Figure 37 displays the detail acquired by a UAS flight and SfM technology to generate an updated mosaic of the wetlands.

Figure 36: Mosaic of mitigation bank on the Hofmann Forest, NC

Chapter 6

6.0 Conclusion

Affordable Unmanned Aerial Systems are an emerging product in today's market that have evolved from being used as a hobby aircraft, into an irreplaceable natural resources inventory tool. This new imagery source can improve overall organization and site management in a way that allows for data to be collected in a safe process that is repeatable and reliable. One may argue that it is easier to implement a simple cruise via a field forester, but UAS applications can be directed to areas where access is limited, or sites that would require additional resources to inventory.

The initial use of having a UAS is the applicability of acquiring and viewing nearly instantaneous remote sensing data. Field foresters can benefit from reconnaissance and monitoring applications using the UAS for 'eyes in the sky' applications. Users with GIS and data processing capabilities can benefit additionally from the post processing of acquired data. Through the use of various highly sophisticated UAS platforms and remote sensing devices we are able to rapidly collect and process up to date data that can be georeferenced in real time. The ability to easily display spatially referenced high resolution photos, orthophotos, or surface models decreases troublesome field time and increases profit margins by allowing for quick and accurate decision making. Displaying UAS data in a GIS program to perform spatial analysis, including area calculation, volume estimation, and 3D modeling can open pathways to business models that did not exist.

And finally, what could be viewed as the best advantage of either fixed wing or multicopter UAS's over manned aircraft remote sensing is safety. Because the pilot is now located on the ground, rather than in the aircraft itself, he or she is not in any danger during the flight. This is especially relevant for dangerous civilian missions, such as observational flights over forest fires with RGB or IR sensors.

6.1 Limitations and future research

As per the FAA regulations, each UAS pilot has to have an FAA UAS license. They are typically bound to fly at 400 feet AGL or below, which limits the area to be inventoried. If the UAS is piloted within five nautical miles of an airport, the pilot is required to notify the appropriate air traffic control tower to allow for increased situational awareness for local manned aircraft. The pilot is also limited by visual line of sight regulations that instruct the pilot or associated observers to physically keep visual contact with an UAS platform at all times. This can restrict the area flown when operated in forested areas or between tall buildings, where the crew is unable to keep unobstructed view of an UAS. While these regulations are set for safety reasons, they limit the capabilities of UAS, as current platforms have the ability to map at greater altitudes due to high-resolution integrated cameras. UAS pilots also have to keep a very close eye on the geographic location of the flights, as any slight change in weather can affect the quality of data. Most platforms are not waterproof, but can fly in considerable amounts of wind. High winds do require more rotor thrust, and decrease the overall time in the air due to battery consumption. While these limitations

restrict usability of UAS to large area applications, cost effectiveness is one of the key drivers that would open pathways for UAS in both research and applications (Canis 2015).

Civil and commercial applications include aerial reconnaissance, search and rescue, survey of forest, timber production, crop production, disaster damage estimation, disaster management, agricultural activities, telecommunications, oil and gas exploration, and geophysical surveys. The ease of UAS deployment will allow repeated mapping at a scale that was previously time and cost consuming, for example, frequent forest survey for the detection of windblown and non-productive areas. Use of SfM technique may drastically change how timber can be inventoried for modeling timber heights. Since repeated surveys and rapid response using UAS are user-friendly, it can be used to quickly access disaster areas for damage assessments and management using 3D mapping. With the aid of high resolution cameras and brushless rotors, visual aid of potentially hazardous areas will increase site awareness without having to place humans in contact with harmful substances (Lin et al., 2013; Ax et al., 2012; Jeziorska et al, 2016). RGB and IR equipped UAS platforms are suitable for the real-time data collection on prescribed or wildfire situations. Lightweight and portable UAS's can be carried by ground crews, and quickly deployed if aerial views are needed to monitor fire movement and direction.

Applicability of UAS will also open doors for both applied and developmental research. For example, it can be used to study Phenological variability due to climate change at broad

scales. While data collection from aircraft is costly, the acquisition date from satellite sensors is dependent upon the orbital characteristics of the platform (Weiss and Baret, 2017). Therefore, capabilities of UAS can help planning flights very close to phenological stages important for detection of plant stress, impact of climate change, or pre-harvest characterization. These UAS flights can be conducted using a variety of sensors such as RGB, multispectral, near-infrared (NIR), hyperspectral, or LiDAR.

References

Berni, J.A.J., Zarco-Tejada, P.J., Suarez, L., & Fereres, E. (2009). Thermal and Narrowband

Multispectral Remote Sensing for Vegetation Monitoring From an Unmanned Aerial

Vehicle. *IEEE Transactions on Geoscience and Remote Sensing, 47*, 722-738

Breckenridge, R.P., Dakins, M., Bunting, S., Harbour, J.L., & White, S. (2011). Comparison

of Unmanned Aerial Vehicle Platforms for Assessing Vegetation Cover in Sagebrush Steppe

Ecosystems. *Rangeland Ecology & Management, 64*, 521-532

Canis, B. (2015). Unmanned aircraft systems (UAS): Commercial outlook for a new

industry. *Congressional Research Service, Washington*

Chiabrando, F., Marenchino, D., Nex, F., Piatti, D., & Rinaudo, F. (2009). Uav Systems for

Photogrammetric Recording in Archaelogical Areas: Problems Suggestions and Products.

Remote Sensing for Environmental Monitoring, Gis Applications, and Geology Ix, 7478

Dandois, J.P., Olano, M., & Ellis, E.C. (2015). Optimal Altitude, Overlap, and Weather

Conditions for Computer Vision UAV Estimates of Forest Structure. *Remote Sensing, 7*,

13895-13920

Goddemeier, N., Daniel, K., & Wietfeld, C. (2010). Coverage Evaluation of Wireless

Networks for Unmanned Aerial Systems. *2010 Ieee Globecom Workshops*, 1760-1765

Themistocleous, K., Ioannides, M., Agapiou, A., & Hadjimitsis, D.G. (2015). The

Methodology Of Documenting Cultural Heritage Sites Using Photogrammetry, UAV And

3D Printing Techniques: The Case Study Of Asinou Church In Cyprus. *Third International Conference on Remote Sensing and Geoinformation of the Environment (Rscy2015), 9535*

Wallace, L., Lucieer, A., Watson, C., & Turner, D. (2012). Development of a UAV-LiDAR System with Application to Forest Inventory. *Remote Sensing, 4*, 1519-1543

Zhou, G.Q., & Zang, D. (2007). Civil UAV system for Earth observation. *Igarss: 2007 Ieee International Geoscience and Remote Sensing Symposium, Vols 1-12*, 5319-+

Appendices

Appendix A

3.01 Abstract - SfM techniques for estimating the volume of wood chips

Volume estimates play a key role in determining the amount of material to be excavated or inventoried in both environmental and civil applications. The process with which these volumes are estimated has traditionally consisted of using standard ground-based surveying techniques. The accuracy of volumetric estimates using traditional methods is resource-intensive and often limited by project timelines, equipment, and available funds. Unmanned aerial systems (UAS) and the miniaturization of remote sensing devices have proved to be cost-effective tools that allow for highly accurate three-dimensional (3D) mapping. The ability to view pairs of hard copy photography in stereo has existed for decades, but thanks to recent structure from motion (SfM) computer programs, multiple pairs of digital photos can be stitched together to generate a corresponding 3D point cloud. If accurate ground control points (GCP) are available, the mosaic can be orthorectified to a spatial accuracy of a few inches. In this study, we collected UAS photographs of wood chip piles for August and September 2016 and processed using 3D volume models generated from multiple SfM programs, and compared them to those collected using a ground survey method. The Pix4D Mapper Pro program outperformed the Agisoft and Maps Made Easy programs. The standard errors were the lowest whereas volume estimates were similar to those of the ground survey. However, the Maps Made Easy application was much simpler and more user-friendly. We also found that the standard error of the wood chip volume decreases as the number of photos

used in the image processing increases. The dataset with the highest number of images had the lowest average standard error.

4.01 Abstract - Applications of UAS technology to monitor Atlantic White-Cedar (AWC) on Hofmann Forest, North Carolina

Species such as the Atlantic white cedar [*Chamaecyparis thyoides* (L.) B.S.P.] (AWC) can thrive in dense, shrubby conditions making it extremely difficult to monitor and study. A means to combat this problem is to use inexpensive unmanned aerial systems (UAS) to inventory and map (via imagery) the regeneration of a young AWC stand located on the Hofmann Forest. This study will provide inventory data on a 30-acre site, which was gathered in minimal time when compared to standard 'boots on the ground' methods.

Appendix B

Agisoft Canopy Height Model limited to 8ft AWC Buffer
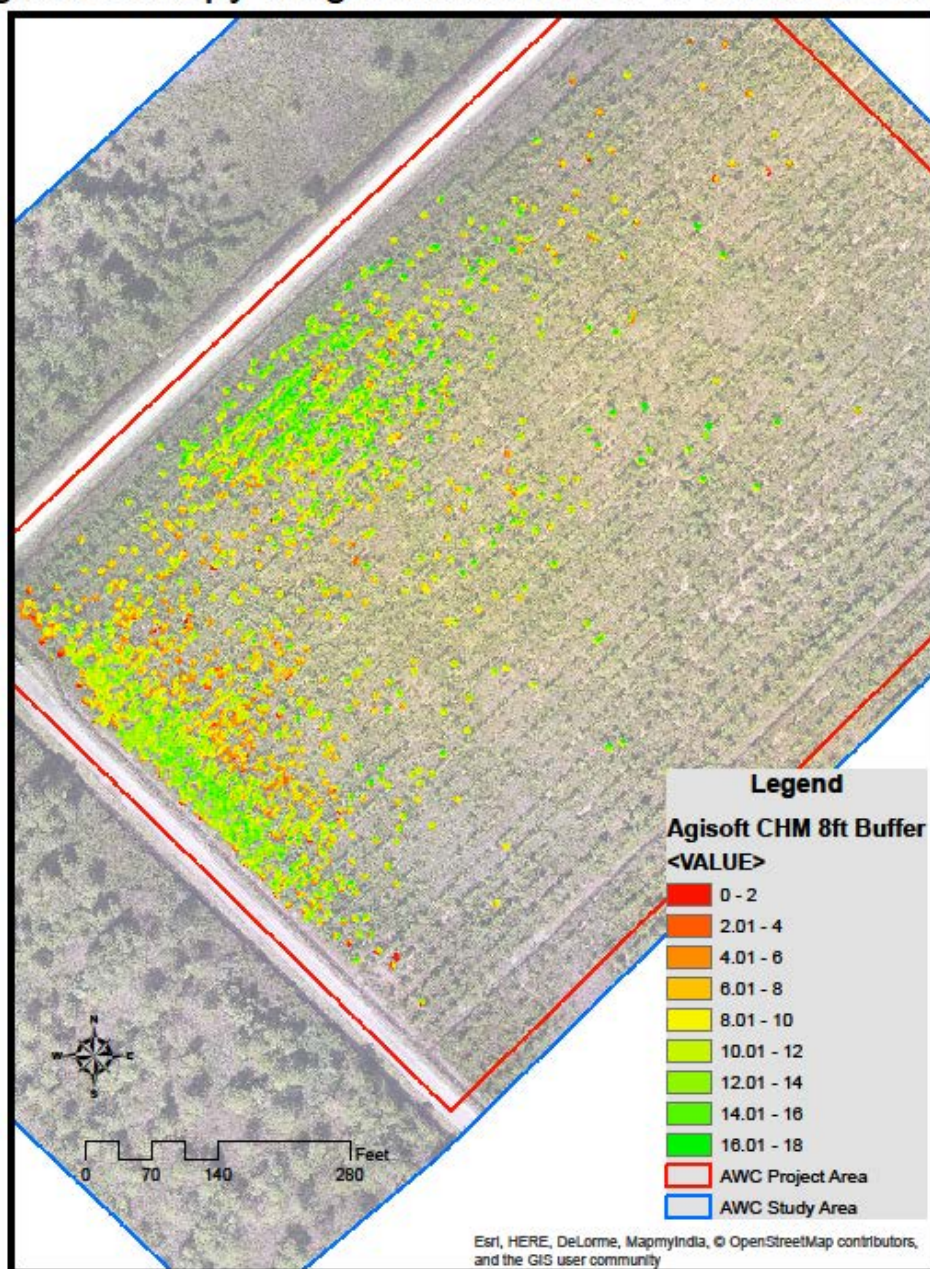
Appendix C
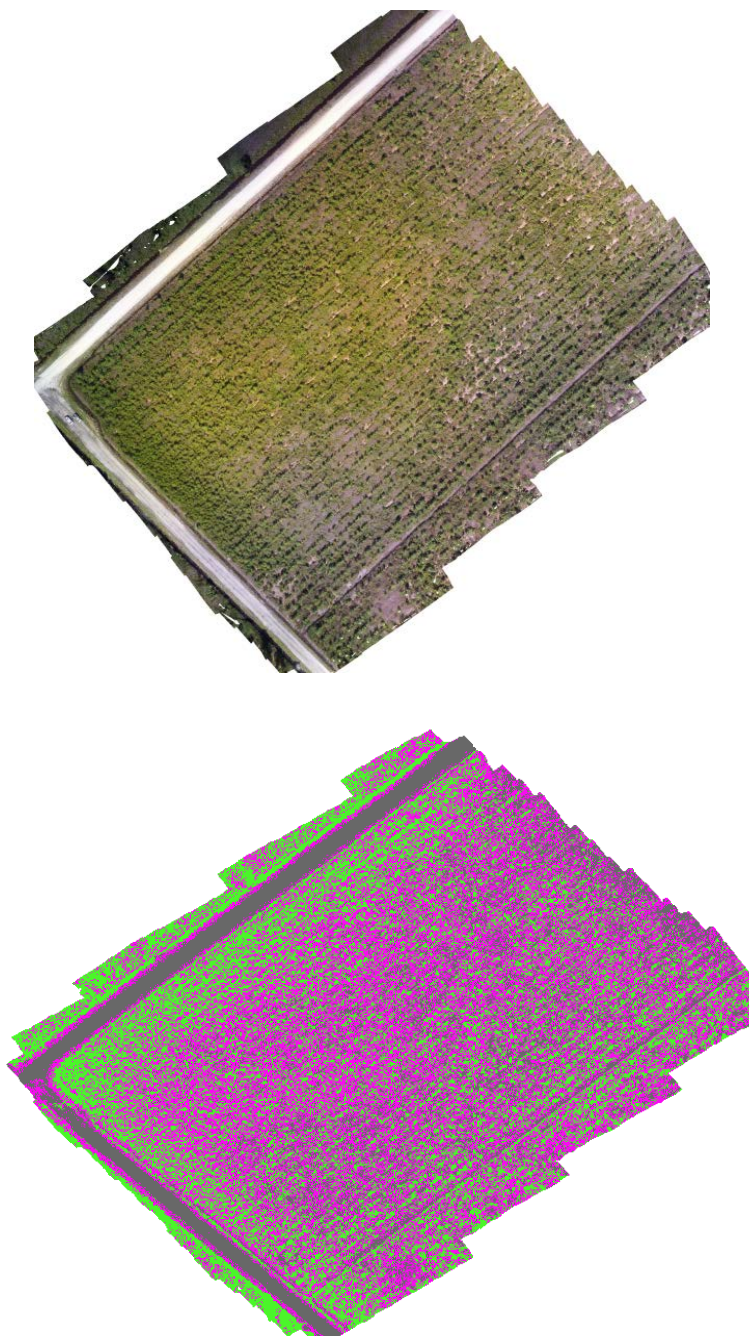
Larger Figure 23: Mosaic (top) and Unsupervised Classification (bottom)